Multiple structure in oxy-hydrogen detonation propagation in rectangular tubes with an improved CE/SE scheme

IOP Conf. Series: Materials Science and Engineering **490** (2019) 062069 doi:10.1088/1757-899X/490/6/062069

Multiple structure in oxy-hydrogen detonation propagation in rectangular tubes with an improved CE/SE scheme

Yang Shen[1], Pu Chen[1] and Deliang Zhang[2,*]

[1]LTCS and College of Engineering, Peking University, Beijing, China
[2]LHD, Institute of Mechanics, Chinese Academy of Sciences, Beijing, China

*Corresponding author e-mail: dlzhang@imech.ac.cn

Abstract. An improved space-time conservation element and solution element (CE/SE) scheme is used to simulate propagation process of 3-D oxy-hydrogen detonation in rectangular tubes. Multiple detonation structure based on elementary cells of the diagonal, rectangular and spinning mode in square tubes are obtained by numerical cases with different aspect ratios of cross-section. By means of visualizing its detailed structure, the formation mechanism of 3-D multiple cellular patterns is preliminarily discussed. As the cross-sectional aspect ratio increases, new multiple cellular patterns are observed.

1. Introduction

Detonation formation and propagation was studied for nearly 100 years. Firstly, people were interested in complex structure in the 3-D detonation propagation. Smoked foil technique was developed in mid-20th century to be a significant experimental method to observe detonation cellular structures. Gradually, it was realized that a numerical model for chemical reaction was rather significant in simulating a whole process of detonation. The detailed reaction model by Oran [1] was a big success to describe the process of energy transformation. Sichel [2] developed Taki's two-step kinetics model [3] using a fitting formula which combined the accuracy of detailed reaction model with the conciseness of ZND models when calculating oxy-hydrogen or air-hydrogen detonation.

At present, the research of 3-D detonation propagation has attracted more and more attention. Hanana [4] successfully did detonation experiments in square tubes and found two kinds of stable propagation structure. Tsuboi [5, 6] repeated Hanana's result by simulation using a high order non-MUSCL scheme and Oran's detailed reaction model. The effective size in Tsuboi's simulation had a lower order of magnitudes than experimental results. Dou [7, 8] and Wang [9, 10] employed one-step chemical model with 5th WENO scheme and obtained the same structure. Furthermore, a new propagation structure namely spinning mode was observed when setting enough small cross-sectional size of square tubes. Moreover, Ivanov [11], Weng[12], Huang [13, 14], Cai [15] and Shen [16] used different numerical scheme and chemical reaction model and came to a similar conclusion.

The CE/SE format is a novel numerical approach for Navier-Stokes equations, which can give consideration to both precision and efficiency. Chang [17] proposed this scheme and extended it to the two-dimensional case [18]. The original division of CEs required fixed distributed grid, which could not be easily extended. Therefore the simplified division of CEs and SEs based on structured grid was made [19] and successfully extended to 3-D computational domains.

This article used an improved CE/SE method with 2nd order Taylor expansion [16] to visualize the 3-D cellular stuctures in rectangular tubes with different cross-sectional aspect ratios. We got the

multiple cellular patterns with different cross-sectional aspect ratios in diagonal, rectangular as well as spinning mode of detonation propagation and discussed their formation mechanism.

2. Numerical conditions

The experimental results show that detonation wave in rectangular ducts has complex 3-D structure, including the front shock wave, transverse wave (TW), Mach stem (MS), incident shock (IS), triple point line (TL), etc. The motion of TLs forms the cellular structure at lateral walls of the tube, which reflects characteristics of the detonation.

In this paper, the effect of different aspect ratios of cross-section (AR) on detonation propagation and cellular structure under the diagonal, rectangular and spinning mode are studied with CE/SE method and Sichel's two-step chemical reaction model [2]. More details about the algorithm description can be found in Ref. [16]. The rest control variables can be set uniformly, as follows.

(1). Initial settings. Oxygen and hydrogen mix as 2:1 mole ratio with pressure $P = 50P_0$ and density $\rho = \rho_0$ at left 5% calculating area as well as $P = P_0$ and $\rho = \rho_0$ in the rest part. Here P_0 = 1atm, T_0 = 298K, $\rho_0 = P_0/RT_0$.

(2). Boundary settings. All the sides of the tube including the front and back walls, are given the reflective boundary.

(3). Grid resolution. Through preliminary calculation, it is confirmed that in cases of the diagonal and rectangular mode, the grid resolution of 25 points per millimeter is appropriate, but in spinning cases, the number had better increase to 50 pts./mm.

(4). Initial perturbation. Internal energy per unit volume $\boldsymbol{e}$ in exothermic reaction zone ($0<\beta<0.99$) is given a small perturbation lasting initial 30 time steps. For the grid point (i, j, k), the $\boldsymbol{e}$ will be corrected if located in exothermic reaction zone and in first 30 time steps, as below.

$$e_{[i,j,k]} = e_{[i,j,k]} \times (1 + \Delta \times (\cos\frac{\kappa\pi(j\delta_y + k\delta_z)}{L_y + L_z} + \cos\frac{\kappa\pi(j\delta_y - k\delta_z)}{L_y + L_z})), \quad (1)$$

$$e_{[i,j,k]} = e_{[i,j,k]} \times (1 + \Delta \times (\cos\frac{\kappa\pi(j\delta_y)}{N_y} + \cos\frac{\kappa\pi(k\delta_z)}{N_z})). \quad (2)$$

Formula (6) and (7) represent initial diagonal perturbation and initial rectangular perturbation, respectively. Parameter $\boldsymbol{\Delta}$ represents the magnitude of the perturbation (herein $\boldsymbol{\Delta}$ = 0.05). Variable δ_y, L_y and N_y stand for the grid size, the length overall and the number of grids in y direction, respectively. Parameter κ controls the number of initial transversal cellular cell. To get one transversal cell we should take κ = 4 in diagonal perturbation and κ = 2 in rectangular perturbation.

(6). Parallel computing. Computational domain of the example is divided averagely along the x direction in parallel running. Adjacent subdomains exchange data of boundary through MPICH library.

3. Results and discussion

In good order to make clear the effect of ARs on detonation propagation in rectangular ducts, it is necessary to carry out typical elementary cells in square tubes. Through appropriate set of initial perturbation and cross-sectional size, we finally get all the typical elementary cellular patterns.

3.1 Typical elementary cells in square tubes

In the examples of square tubes, the diagonal mode is observed at cross-section size of 4 mm ($L = L_y = L_z$ = 4 mm) with initial perturbation made by Formula (6) when κ = 4, the rectangular mode is observed at the same cross-section size with initial perturbation made by Formula (7) when κ = 2, and the spinning mode is observed at cross-section size of 1 mm ($L = L_y = L_z$ = 1 mm) with initial perturbation made by Formula (6) when κ = 4, or by Formula (7) when κ = 2, as shown in (a), (b), (c), (d) of Figure 1. In the propagation process of detonation with initial perturbation, transverse waves (TWs) split the leading shock wave into several triple point lines (TLs). Because of the motion of TLs, cellular pattern will take shape on side walls, being scale shape in the rectangular and diagonal mode, or parallel stripes in the spinning mode.

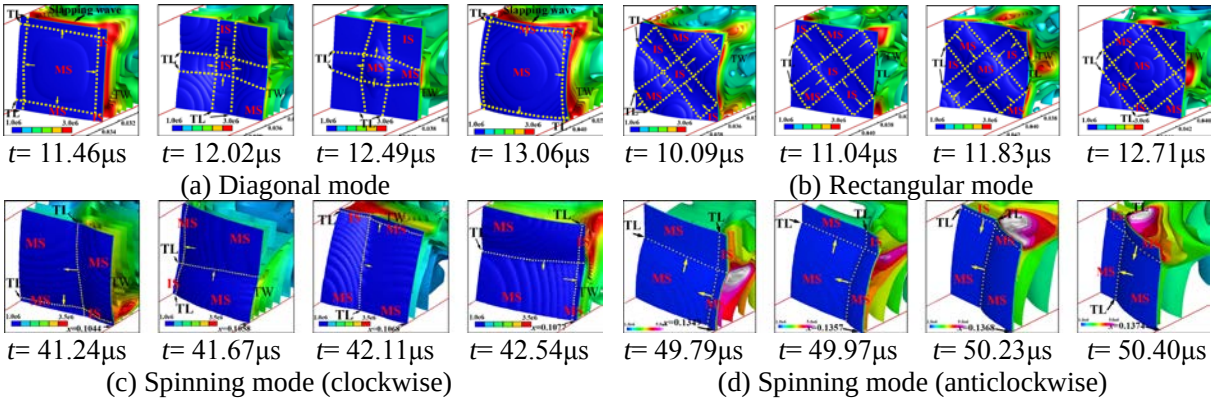

Figure 1. Pressure isosurfaces in about one period when simulating with different initial perturbation and cross-sectional size L, including (a) the diagonal mode (Formula 6 with κ= 4, L= 4 mm), (b) the rectangular mode (Formula 7 with κ= 2, L= 4 mm), (c) the spinning mode (Formula 6 with κ= 4, L= 1 mm, clockwise), and (d) the spinning mode (Formula 7 with κ= 2, L= 1 mm, anticlockwise).

In spinning mode shown in Figure 1(c) and 1(d), the intersection of two TLs spirals on the contrary direction, which depends on types of initial perturbation. In the next chapter, we will find increasing ARs based on these two kinds of spinning cells will form different multiple structure.

3.2 Influence of ARs in the diagonal mode

First of all, the elementary cell with side length L= 4 mm and initial diagonal perturbation is stretched and discussed. In the cases shown in Figure 2, all conditions are equal, but only AR ranges from 1 to 3.

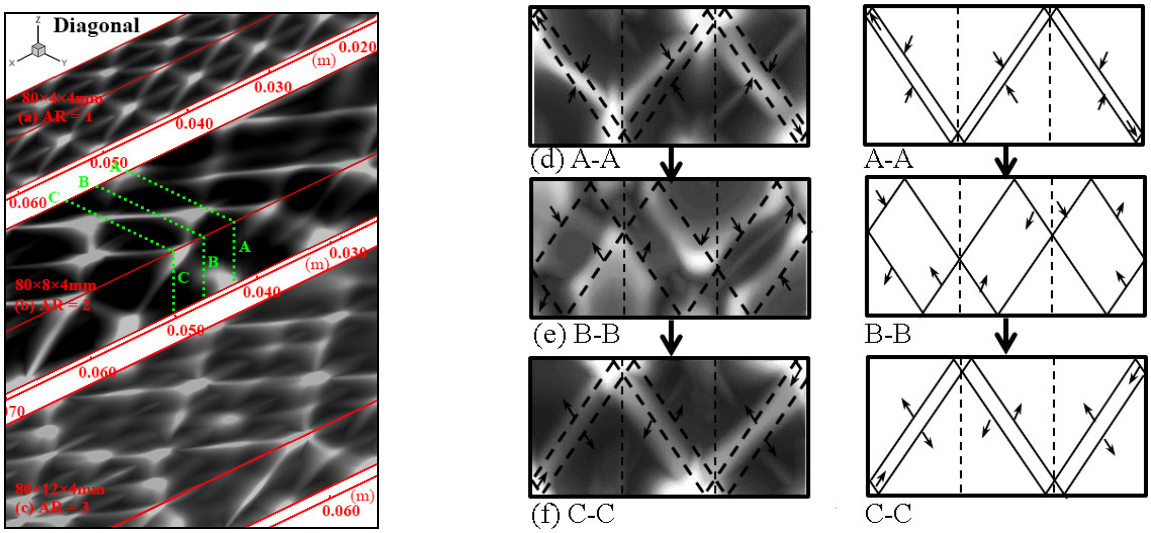

Figure 2. Cellular structure when setting different ARs, with initial diagonal perturbation and elementary cell size L = 4mm, including (a) AR = 1, (b) AR = 2, (c) AR = 3, and Section (d) A-A, (e) B-B as well as (f) C-C of (b).

Generally speaking, if the long side of the rectangular tube stretches a little, the elementary cellular patterns just prefer stretching its corresponding direction. However, when the long side of the rectangular tube doubles or more, the multiple cellular structures have to produce more TLs and elementary cells to fit the rectangular duct. Moreover, the relationship between changing tubes and multiple cellular structures are not simply double and duplicate. Sometimes the stretching of the long side will make influence in the short one, as shown in Figure 2(b), in which half of TLs disappear.

Figure 2(d), 2(e) and 2(f) clearly show distribution of MPHs (maximum pressure histories) on slices A-A, B-B and C-C. It's obviously a compressed triple structure and losses a half number of TLs, that means missing its axial symmetry.

3.3 Influence of ARs in the rectangular mode

Similarly, simulation results shown in Figure 3 are composite patterns based on the rectangular elementary cell with side length L= 4 mm as well.

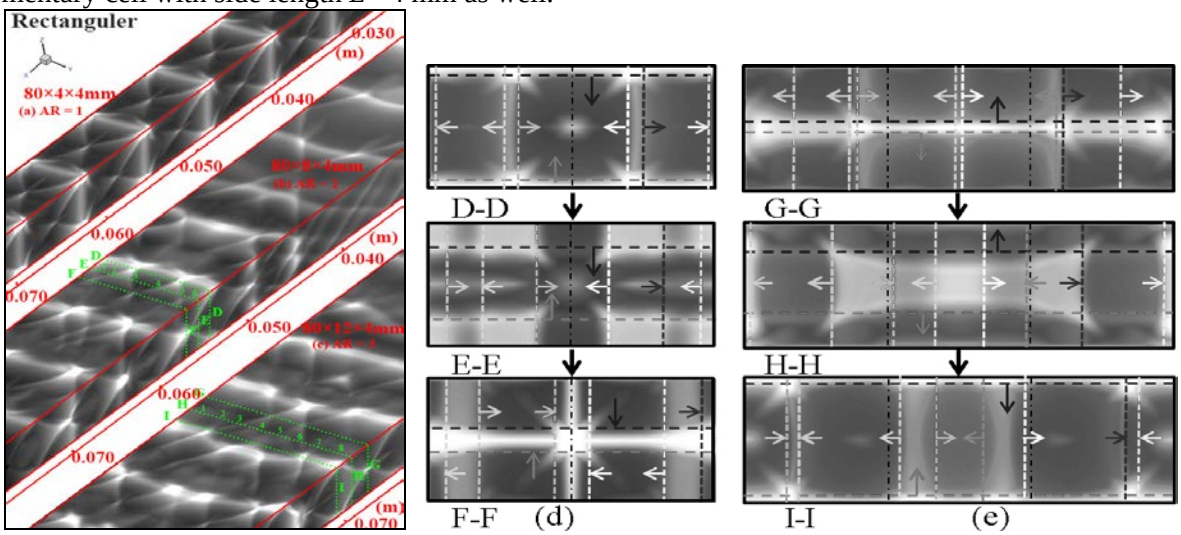

Figure 3. Cellular structure when setting different ARs, with initial rectangular perturbation and elementary cell size L = 4mm, including (a) AR = 1, (b) AR = 2, (c) AR = 3, (d) Section D-D, E-E, F-F of (b) and (e) Section G-G, H-H, I-I of (c).

First of all, the short side of the rectangular tube will not degenerate to a half cell because of the moving style in this mode. Additionally, TLs parallel to the longer side walls in the multiple structure are linked together, leading to longer slapping waves appear in this composite structure.

Figure 3(d) and 3(e) give a visualized picture of motion of TLs in composite structures. As the number of AR increases, it is more difficult to keep the same moving phase and the long slapping wave, resulting in a bigger curvature. However, the motion of TLs still follows axial symmetry.

3.4 Influence of ARs based in the spinning mode

It makes quite different when the cross-sectional size decreases into spinning mode. At first, we discuss the composite structure with initial diagonal disturbance as well as AR = 2.

Figure 4 shows MPHs in half a cycle in this case. As the shock front go forward, three TLs intersect at A1, A2, B1, B2 and C1, C2 on the boundary. Observing the motion of intersection points, we find this multiple cellular structure is composed of double spinning modes with clockwise and anticlockwise rotating directions. If visualizing on the front direction, the clockwise spinning always locates at the right half. In the next case, we will obtain the opposite multiple structure with initial rectangular perturbation.

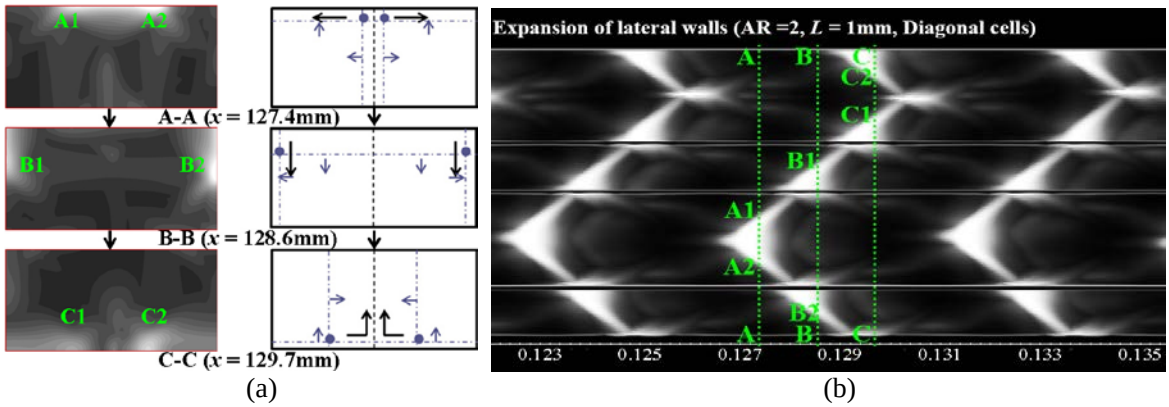

(a) (b)

Figure 4. MPHs in case with initial diagonal disturbance, AR= 2 and L= 1 mm, including (a) expansion of lateral walls and (b) typical Y-Z slices.

If given initial rectangular disturbance at the beginning with enough small cross-sectional size, the composite structure will change a lot, as shown in Figure 5.

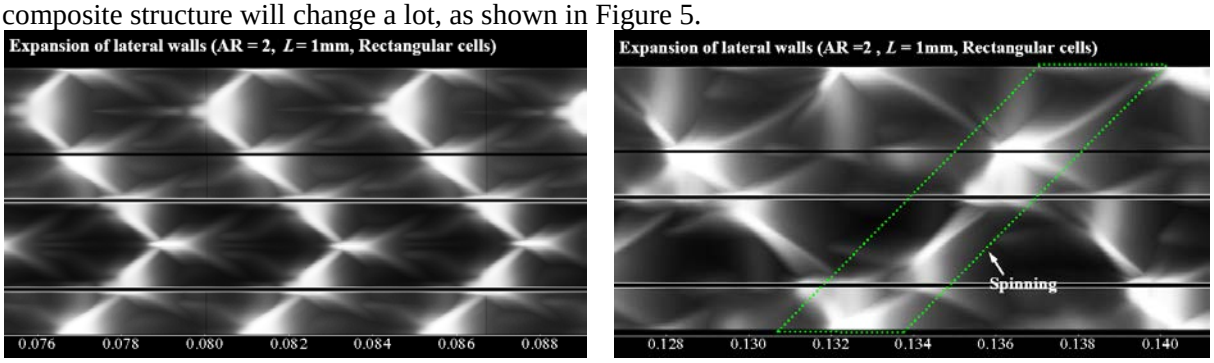

(a) (b)

Figure 5. Cellular structure on side walls in case with initial rectangular perturbation, AR= 2 and L= 1 mm, where x ranges from (a) 0.075 m to 0.089m, and (b) 0.127 m to 0.141m.

Visualizing the MPHs on lateral walls in Figure 5(a), the composite structure becomes quite same with pictures in Figure 4(b). The most obvious difference is the combination mode of spiral directions. However, in the latter 1/4 computational area, the MPHs on the long sides lose its axial symmetry, which show the similar pattern as in half an elementary cells, as shown in Figure 5(b).

Figure 6 give a direct visualization of appropriate cutting slices in x-axis direction, showing how the remain two TLs move in this case. Coincidentally, we also find two opposite moving type of TLs in one example, as shown in (a) and (b) below.

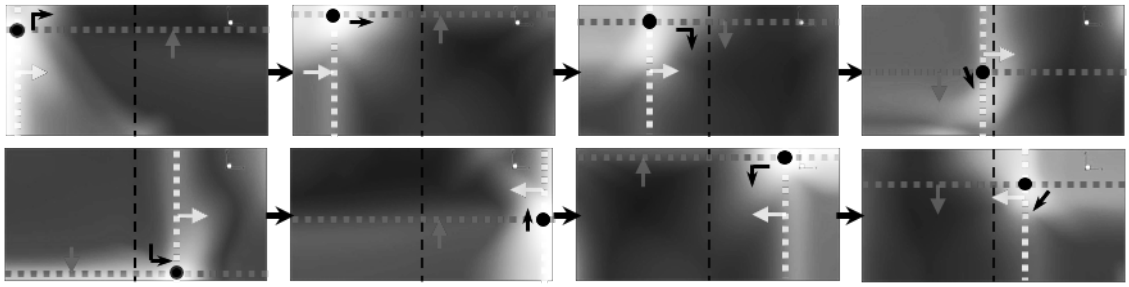

(a) One type of motion of TLs

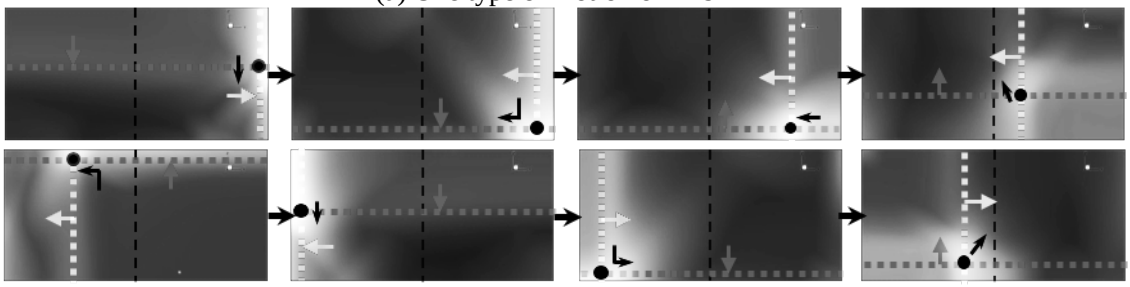

(b) The other type (opposite)

Figure 6. Motion of TLs in latter 1/4 domain in case with initial rectangular perturbation, AR= 2 and L= 1 mm, where x ranges from (a) 0.119 m to 0.125m, and (b) 0.138 m to 0.144m.

In this condition, one of the two short TLs disappear in the latter 1/4 computational area. If following the original moving style, the remain short TL will move more slowly than the long TL, which makes the intersection of these two TLs look like moving along '∞' lines. However, we find in some cycles the short TL will move with the double velocity. In these cycles, MPHs on the side walls will appear similar with pictures in spinning modes, as shown in Figure 5(b). That's the reason two types of moving styles of TLs will exist in just one example.

3.5 Influence of high ARs

Previous experiments about 2-D detonation always built rectangular ducts with a high AR. Therefore, the detonation cellular patterns in numerical examples with high ARs are certainly similar to pictures in 2-D detonation. The truth is as we think. Figure 7 shows MPHs in case with initial rectangular disturbance, AR = 4 and L = 1 mm. It is obvious that the pressure has changed little in z-axis direction, and makes a standard distribution as in 2-D condition.

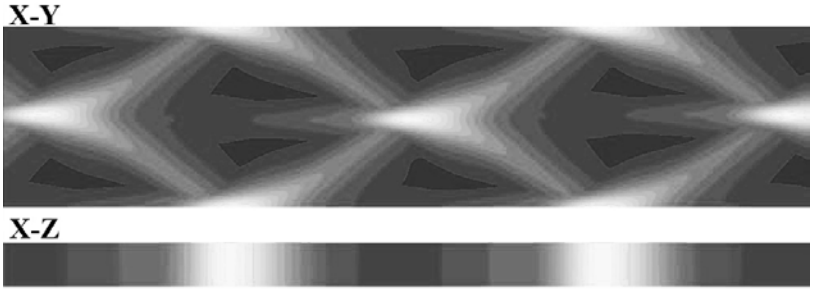

Figure 7. Cellular structures on side walls with initial rectangular disturbance, AR= 4 and L= 1 mm

4. Conclusion

In this article, we chiefly discuss the composite structures of oxy hydrogen detonation when giving different cross-sectional aspect ratios with an improved CE/SE method with 2nd order Taylor expansion and Sichel's two-step chemical reaction model. Ultimately, it is demonstrated that composite cellular patterns will almost be made up of elementary units in the square tubes with stretching or duplicating. When cross-sectional aspect ratio decreases to 1 or given an enough high value, the cellular structure will transform to the elementary cells or 2-D patterns, what we are familiar with.

References

[1] E. S. Oran, J. W. Weber, E.I. Stefaniw, et al., A numerical study of a two-dimensional H_2-O_2-Ar detonation using a detailed chemical reaction model, Combustion and Flame, 1998, 113 , pp. 147-163.
[2] M. Sichel, N. A. Tonello, E. S. Oran, et al., A two-step kinetics model for numerical simulation of explosions and detonations in H_2-O_2 mixtures, Proceedings of The Royal Society of London Series A-Mathematical Physical and Engineering Sciences, 2002, 458 (2017), pp. 49-82.
[3] S. Taki, T. Fujiwara, Numerical Analysis of two-dimensional nonsteady detonations, AIAA Journal, 1978, 16(1), pp. 73-77.
[4] M. Hanana, M. H. Lefebvre, P.J. Van Tiggelen, Pressure profiles in detonation cells with rectangular and diagonal structures, Shock Waves, 2001, 11, pp. 77-88.
[5] N. Tsuboi, S. Katoh, A. K. Hayashi, 3-D numerical simulation for hydrogen/air detonationpp. rectangular and diagonal structures, Proceedings of the Combustion Institute, 2002, 29, pp. 2783-2788.
[6] N. Tsuboi, M. Asahara, K. Eto, et al., Numerical simulation of spinning detonation in square tube, Shock Waves, 2008, 18, pp. 329-344.
[7] H. S. Dou, H. M. Tsai, B. C. Khoo, et al. Simulations of detonation wave propagation in rectangular ducts using a 3-D WENO scheme, Combustion and Flame, 2008, 154, pp. 644-659.
[8] H. S. Dou, B. C. Khoo, Effect of initial disturbance on the detonation front structure of a narrow duct, Shock Waves, 2010, 20(2), pp. 163-173.
[9] C. Wang, C. W. Shu, W. H. Han, et al., High resolution WENO simulation of 3D detonation waves, Combustion and Flame, 2013, 160, pp. 447-462.
[10] C. Wang, P. Li, Z. Gao, et al., 3-D detonation simulations with the mapped WENO-Z finite difference scheme, Computers and Fluids, 2016, 139, pp. 105-111.
[11] M. F. Ivanov, A. D. Kiverin, I. S. Yakovenko, et al., Hydrogen oxygen flame acceleration and deflagration to detonation transition in 3-D rectangular channels with no-slip walls, Int. J. Hydrogen Energ., 2013, 38(36), pp. 16427-16440.

[12] C. S. Weng, J. P. Gore, A numerical study of two- and 3-D detonation dynamics of pulse detonation engine by the CE/SE method, Acta Mech. Sinica, 2005, 21(1), pp. 32-39.
[13] Y. Huang, H. Ji, F. S. Lian, et al., 3-D parallel simulation of formation of spinning detonation in a narrow square tube, Chinese Physics Letters, 2012, 29(11), pp. 114701
[14] Y. Huang, H. Ji, F. S. Lian, et al., Numerical study of 3-D detonation structure transformations in a narrow square tube from rectangular and diagonal modes into spinning modes, Shock Waves, 2014, 24, pp. 375-392.
[15] X. D. Cai, J. H. Liang, R. Deiterding, et al. Adaptive mesh refinement based simulations of three dimensional detonation combustion in supersonic combustible mixtures with a detailed reaction model, Int. J. Hydrogen Energ., 2016. 41(4), pp. 3222-3239.
[16] Y. Shen, H. Shen, K. X. Liu, et al., Three-dimensional detonation cellular structures in rectangular ducts using an improved CE/SE scheme, Chinese Physics B, 2016, 25(11), pp. 114702.
[17] S. C. Chang, The method of space-time conservation element and solution element-A new approach for solving the Navier-Stokes and Euler equations, Journal of Computational Physics, 1995, 119, pp. 295-324.
[18] S. C. Chang, X. Y. Wang, C. Y. Chow, New developments in the method of space-time conservation element and solution element — Applications to two-dimensional time-marching problems, NASA/TM, 1994, 106758.
[19] M. Zhang, S. T. Yu, S. C. Chang, Solving the Navier-Stokes equations by the CE/SE method, AIAA, 2004, 2004-0075.